

Color Photographs of an Accretion Disk around a Black Hole

Jun FUKUE

Astronomical Institute, Osaka Kyoiku University, Tennoji-ku, Osaka 543

and

Takushi YOKOYAMA

Jyoto Junior High School, Jyoto-ku, Osaka 536

(Received 1987 June 29; accepted 1987 October 23)

Abstract

Color photographs of a geometrically thin relativistic accretion disk around a Schwarzschild black hole are obtained and displayed. Photographs in optical and X-ray wavelengths as well as a bolometric picture are also obtained and compared with one another. When the temperature at the inner region of the disk is some 10^7 K, the X-ray and bolometric images are rather contrasty, while the brightness of the disk in the optical image gradually decreases from the inner region toward the fringe. X-ray light curves when the relativistic accretion disk is eclipsed by its companion are calculated. It is demonstrated that light curves exhibit asymmetric profiles due to the relativistic Doppler effect by the disk rotation. This light curve asymmetry inherent in the relativistic disk provides an alternative strategy to search for and detect the accretion disk around a compact object. Such an observation will verify the disk model and bring the space-time information near the compact object.

Key words: Accretion disks; Black holes; Light curves; Photometry; X-ray astronomy.

1. Introduction

Two decades have passed since the concept of accretion disk appeared in astrophysics (Lynden-Bell 1969; Shakura and Sunyaev 1973; Novikov and Thorne 1973). Since then, however, it has not easily shown its face. Hence, it is quite natural that people would want to observe it.

The first attempt to visualize the accretion disk around a black hole was made by Luminet (1979). He obtained a simulated “bolometric photograph” of the disk, and therefore the photograph displayed is monochromatic. Thus one of the aims of this paper is to take a color picture of the disk. In addition, the X-ray and optical photographs are compared with the bolometric photograph. These photographs give not only the disk’s portrait but also several astrophysical suggestions on a black-hole-accretion disk system.

To date, the possibility of observing accretion disks around compact objects has been investigated mainly in relation to their spectra. For instance, the spectrum from the entire disk superposed by blackbodies with different temperature (Shakura and Sunyaev 1973) was detected by the X-ray astronomical satellite *Temma* and called a multicolor spectrum (Mitsuda et al. 1984). Czerny et al. (1986) also discussed the illuminating effect by the central neutron star on the spectrum from the neutron star-accretion disk system. Cunningham (1975) calculated the spectrum from a relativistic accretion disk surrounding the Kerr black hole. The ultraviolet excesses in the spectra of several quasars are interpreted by his model (Malkan 1983). Finally, Gerbal and Pelat (1981) studied line profiles emitted by an accretion disk and derived the asymmetric, double-peaked profiles.

An alternative strategy to detect the relativistic accretion disk is suggested by Fukue (1987b). The radiation from the accretion disk suffers from a significant Doppler shift due to the disk rotation. As the blue- or red-shift is strongest in the inner region where most light comes from, the total flux is affected by this relativistic (de)-boost. That is, light curves during an eclipse of the disk will exhibit asymmetric profiles. He pointed out this asymmetric feature of light curves inherent in the relativistic disk, using a very simple model where the entire disk is divided into two parts: the blueshifted semicircle and the redshifted one. In the present paper, we calculate the light curve more precisely in terms of the photographs taken. Such a photometric approach as well as a spectroscopic one is useful for the observational study of an accretion disk.

In the next section, the method to take a photograph is explained. Several photographs are displayed and their properties are discussed in section 3. X-ray light curves calculated from the present results are given in section 4.

2. Method of Taking a Photograph

In this section, we describe the method of taking a photograph of an accretion disk.

a. Arrangement

As a central gravitating object of the accretion disk, we have chosen a black hole of mass M , because the black hole is the simplest collapsed body in comparison with other objects such as a neutron star. Our target is a Schwarzschild black hole as in the case studied by Luminet (1979), although almost all the black holes in the universe may be Kerr black holes.

The main subject, the accretion disk around the hole, is a geometrically thin disk. Because of the relativistic effect, the disk has an inner edge at the marginally stable radius, which equals three Schwarzschild radii in the present situation.

The photographer is located at (r_0, δ_0) , where r_0 is the photographer's distance from the center in the Schwarzschild coordinates (r, θ, φ) and $\delta_0[=(\pi/2)-\theta_0]$ is the declination angle. In contrast, Luminet (1979) set the observer at infinity. Finally, the accretion disk rotates counterclockwise against the line of sight of the photographer.

This arrangement is schematically shown in figure 1.

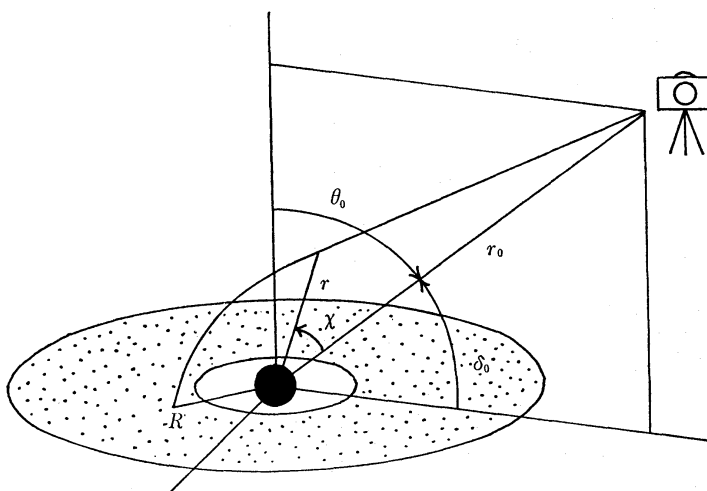


Fig. 1. Schematic view of the photographer and the subjects: the geometrically thin accretion disk and the Schwarzschild black hole. In the central region of the disk, there is a hole around the hole. The disk extends toward the outer region infinitely. The photographer is located at (r_0, θ_0) . The light ray travels from the disk to the photographer along the null geodesics and vice versa.

b. Trajectory

The photon emitted from some point on the disk travels along the null geodesics to be received by the observer (or to expose a film). In the present case, however, the light ray is traced from the photographer to the point where it originates based on Fermat's principle. The path of a light ray is determined by the well-known equation:

$$\frac{d^2}{d\chi^2} \left(\frac{1}{r} \right) = -\frac{1}{r} + \frac{3}{2r^2}, \quad (1)$$

where r is the distance from the center and χ is the angle measured from the direction of the photographer (see figure 1). The Schwarzschild radius $r_g = 2GM/c^2$ is set to be unity in equation (1).

Moreover, only the direct image was obtained and the secondary or higher order images are neglected, since they have little influence on the photographic image (Luminet 1979).

c. Observed Flux and Observed Temperature

In the standard model of geometrically thin relativistic disks (e.g., Page and Thorne 1974), the bolometric flux of radiation from the disk is given by

$$F = \frac{3GM\dot{M}}{8\pi r_g^3} \frac{1}{(R-3/2)R^{5/2}} \left[R^{1/2} - 3^{1/2} + \frac{(3/2)^{1/2}}{2} \ln \frac{R^{1/2} + (3/2)^{1/2}}{R^{1/2} - (3/2)^{1/2}} \frac{3^{1/2} - (3/2)^{1/2}}{3^{1/2} + (3/2)^{1/2}} \right], \quad (2)$$

where R is the radial distance from the center in the equatorial disk plane and measured in units of the Schwarzschild radius and \dot{M} is the accretion rate.

The temperature of the disk is then obtained by the relation

$$T = (F/\sigma)^{1/4}, \quad (3)$$

where σ is the Stefan-Boltzmann constant.

Since the flux is maximum at about $R=4.8r_g$ and vanishes at $R=3r_g$ (the inner edge) in the standard model, the temperature behaves in the same way.

Instead of the mass or the accretion rate, we use the maximum temperature T_{\max} of the disk at $\sim 4.8r_g$ as a parameter. From equations (2) and (3), we have $\sigma T_{\max}^4 = 0.000917 \times 3GM\dot{M}/(8\pi r_g^3)$. Inserting the numerical values, we finally obtain the relation

$$T_{\max} = 10^7 \dot{M}_{18}^{1/4} M_0^{-1/2} \text{ K}, \quad (4)$$

where \dot{M}_{18} and M_0 are respectively the accretion rate in units of 10^{18} g s^{-1} and the mass of the central black hole in units of $1M_\odot$.

As is well known, the observed bolometric flux F_{obs} as well as the observed temperature T_{obs} are changed due to the relativistic effect as

$$F_{\text{obs}} = F/(1+z)^4, \quad (5)$$

$$T_{\text{obs}} = T/(1+z), \quad (6)$$

where z is the redshift which consists of the Doppler effect against the photographer by the rotation of the disk gas and of the gravitational redshift by the existence of the black hole (Luminet 1979). This redshift is determined by Luminet's (1979) equation (19).

d. Parameters

The parameters under the present situation are ultimately the photographer's distance r_0 , his declination angle δ_0 , and the maximum temperature T_{\max} of the disk, besides the technical ones such as the view area or f-number.

Of these the photographer is always located at $r_0 = 10^4 r_g$. Furthermore, there are two cases for the maximum temperature: $T_{\max} = 10^7 \text{ K}$ and $T_{\max} = 10^4 \text{ K}$. The former is associated with the accretion disk surrounding the black hole of stellar size as in some of the galactic X-ray sources, whereas the latter is of the disk of somewhat cooler type existing in active galactic nuclei.

3. Photographs of the Accretion Disk

Now let us exhibit a few photographs of the geometrically thin accretion disk.

In figure 2 several types of the photograph of the same disk from the same angle are displayed. The parameters characterizing the situation are $r_0 = 10^4 r_g$, $\delta_0 = 20^\circ$, and $T_{\max} = 10^7 \text{ K}$ (i.e., the disk rotates around a stellar-mass black hole). In addition, the other photographing parameters are as follows: the view area is $30r_g$ across, the f-number is 8, and the shutter speed is 0.5 s. The mesh size is 201×201 and the resultant maximum resolution is about $0.15r_g$.

Figure 2a shows the distribution of the observed temperature T_{obs} which is expressed in false color. From orange through yellow and white to blue, the observed temperature increases in steps of 10^6 K . The border of the central black region is the inner edge of the disk where the brightness of the disk abruptly drops. The ap-

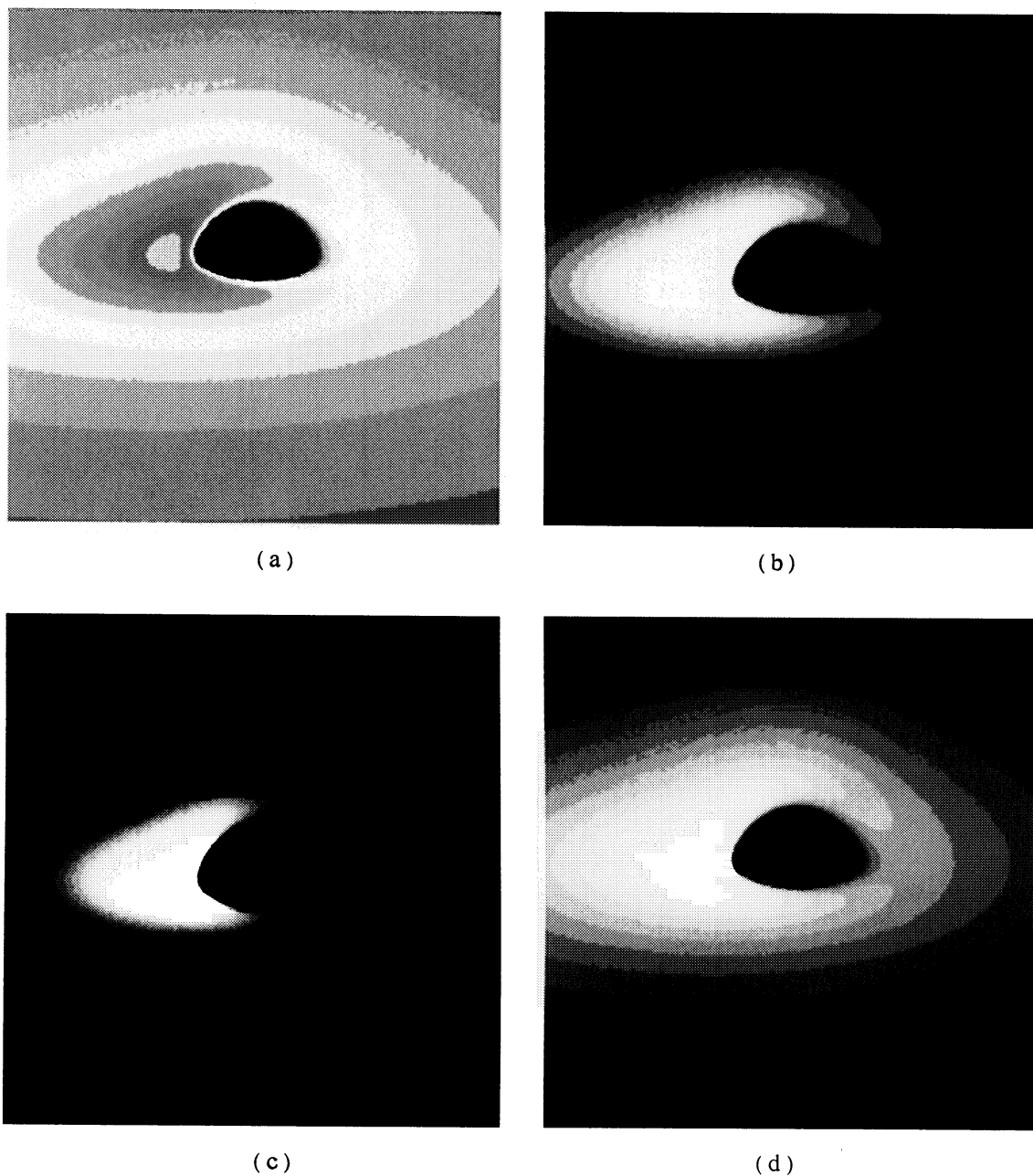


Fig. 2. Several types of the photograph of the disk with $T_{\text{max}} = 10^7$ K rotating around a stellar-mass black hole. The photographer's distance from the center is $10^4 r_g$ and his declination angle is 20° . Furthermore, he has taken a photograph in the region of $30 r_g$ across with resolution $\sim 0.15 r_g$. (a) The distribution of the observed temperature in false color. From orange ($T_{\text{obs}} < 3 \times 10^6$ K) through yellow ($4 \times 10^6 \text{ K} < T_{\text{obs}} < 5 \times 10^6$ K) and white ($6 \times 10^6 \text{ K} < T_{\text{obs}} < 7 \times 10^6$ K) to violet ($T_{\text{obs}} > 1.2 \times 10^7$ K), the observed temperature increases in steps of 10^6 K. (b) The bolometric photograph. (c) The X-ray photograph in the 2–30-keV band. (d) The optical photograph in the 0.38–0.77- μm band.

parent size of this region is somewhat larger than the simple projected size because of the gravitational lens effect. Figure 2a is essentially the same as the contour map of the total flux given by Luminet (1979).

Figures 2b, 2c, and 2d are respectively bolometric, the X-ray, and the optical photographs through a monochromatic filter. In each picture an appropriate filter is chosen so as to avoid both an overexposure at the brightest region and an underexposure at the fringe. Of these, figure 2b, the bolometric photograph, is the same type of photograph taken by Luminet (1979). In figure 2c the X-ray wavelength band is taken as 2–30 keV, bearing in mind the large-area proportional counter (LAC) aboard the X-ray astronomical satellite Ginga (see the next section). On the other hand, in figure 2d the optical wavelength taken is from $0.38\ \mu\text{m}$ to $0.77\ \mu\text{m}$.

These images are significantly distorted by the Doppler effect associated with the disk rotation and by the gravitational bending of the light ray near the black hole as already discussed by Luminet (1979). That is, the emergent radiation from the left part of the image which is approaching the photographer with relativistic speed near the black hole is remarkably enhanced by the Doppler shift, while the right part is reduced. This is the reason why the image is asymmetric in the horizontal direction. Since the disk rotation is relativistic Keplerian, the Doppler (de)boost is effective in the inner region of the disk. Moreover, the light ray originating from the opposite side of the disk is strongly bent by the gravity of the black hole before it reaches the photographer. This is the reason why the image is asymmetric in the vertical direction.

In addition to these asymmetric appearances of the disk, we further append several properties on its appearance.

At a glance, we can find the fact that the brightness in the bolometric and the X-ray photographs quickly drops from the inner region to the outer region. Hence these photographs are rather contrasty. On the contrary, the brightness in the optical photograph gradually decreases toward the fringe. Therefore the contrast is weak and the optical image looks like a bright square with a dark hole.

These are understood as follows. The temperature of the standard disk roughly varies as $T \propto R^{-3/4}$ [cf. equations (2) and (3)]. Without the relativistic effect the observed bolometric flux is proportional to T^4 and therefore depends on R as R^{-3} . Hence it quickly drops toward the outer region and this is the reason why the photographs in the bolometric flux is contrasty. Furthermore, since the peak of the blackbody spectrum with temperature $10^7\ \text{K}$ is 2.4 keV, the X-ray photograph in the 2–30-keV band is similar to the bolometric image.

On the other hand, the optical wavelengths of $0.38\text{--}0.77\ \mu\text{m}$ fall in the Rayleigh–Jeans part of the spectrum in the present case. Therefore, the flux integrated in the optical region depends linearly on T . Thus the optical flux varies as $R^{-3/4}$ and consequently the contrast of the optical photograph becomes weak in comparison with that of the bolometric picture.

In figure 3 a color photograph taken in the visual band is also displayed. The parameters in figure 3 are $r_0 = 10^4 r_g$, $\delta_0 = 5^\circ$, and $T_{\text{max}} = 10^4\ \text{K}$. Such a disk is of the type expected to surround a supermassive black hole in active galactic nuclei. We note that this photograph has been taken out of focus artificially.



Fig. 3. The color photograph of the disk located at the center of active galaxies. This seems to be its best photogenic side.

Since the original spectrum from the disk is continuum blackbody radiation, the observed one is not so colorful. For example, we cannot expect blue, green or violet. However, as seen in figure 3, the color gradually changes from brilliant white in the inner brightest region through yellow and orange to dark red in the outer region. Furthermore, unlike figure 2d which is an optical photograph of the high temperature disk, figure 3 is contrasty, since the peak of the spectrum is now in the optical region. This seems to be the best photogenic side of the disk.

4. Light Curves

As shown in the previous section, the special feature of a relativistic accretion disk around a compact object is its asymmetric appearance. That is, the image becomes asymmetric in the vertical direction due to the gravitational lens effect of the central object, and also becomes asymmetric in the horizontal direction due to the Doppler effect associated with the disk rotation. This asymmetric shape becomes more prominent when we observe the disk with smaller declination angle (or larger inclination angle). This is reflected in their spectra (Cunningham 1975). Is there anything else?

The accretion disk can be eclipsed by other objects; for example, by the companion stars in close binary systems or by the gas clouds in active galactic nuclei. It is expected that ingress and egress of light curves observed during eclipse of the disk become asymmetric, as already pointed out by Fukue (1987b). He discussed the light curve asymmetry, using a very simple model. Here we calculate light curves more precisely, using the results obtained in the previous section.

We assume that the object eclipsing the disk moves in its orbit in the same sense as the disk rotation. Hence, the approaching part of the disk is first occulted and then the receding part is. Furthermore, the disk is assumed to be eclipsed by the obstacle with vertical edge in the printed plane.

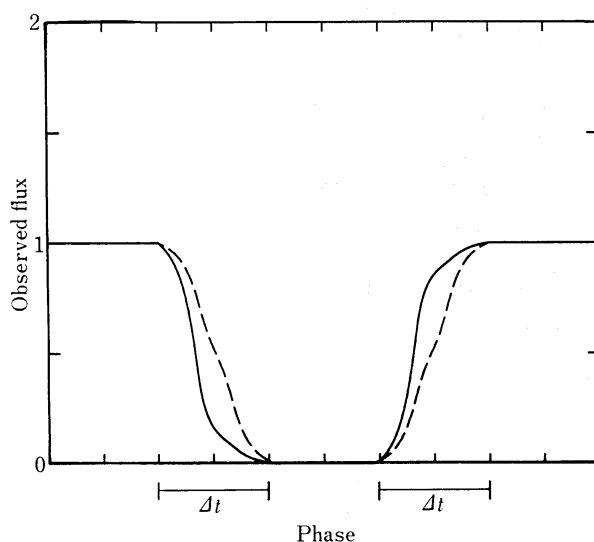


Fig. 4. The X-ray light curves of the disk with $T_{\max}=10^7$ K during an eclipse. The declination angle of the observer is assumed to be 30° . The solid curve represents the light curve of the relativistic disk, while the dashed one denotes that of the disk without rotational and gravitational effects. The asymmetric profile clearly distinguishes the former from the latter.

a. Close Binary Systems

Let us first suppose the accretion disk around a compact star in close binary systems with maximum temperature of 10^7 K. Hence the peak of the spectrum falls in the X-ray region.

Figure 4 shows an example of X-ray light curves in the 2–30 keV band. The declination angle is $\delta_0=30^\circ$. In figure 4, the solid curve represents the expected X-ray light curve of the relativistic disk, while the dashed one denotes that of a hypothetical disk where the effects of rotation and gravitation are neglected. The former shows the *asymmetric feature* as expected, although the latter is symmetric. This asymmetry in light curves is one of the most prominent features of the relativistic accretion disk around a compact object.

The dependence of X-ray light curve on the declination angle is shown in figure 5. In figure 5, from top to bottom, the declination angle is $\delta_0=90^\circ$ to 10° in steps of 10° . Of course, the larger declination angle will not be realized in the close binary system unless the disk plane inclines to the orbital plane.

It should be noted that, in the optical light curves of the disk with $T_{\max}=10^7$ K, the asymmetric feature is not so impressive, because the disk is entirely bright as seen in figure 2d.

As already discussed in Fukue (1987b), the eclipsed time scale Δt is roughly estimated as

$$\Delta t = 0.0427 R a^{1/2} M_1 (M_1 + m_1)^{-1/2} \text{ s}, \quad (7)$$

where R is the size of eclipsed region in units of the Schwarzschild radius, a is the orbital separation in units of the solar radius, and M_1 and m_1 are respectively the black hole mass and the companion mass in units of ten solar masses. Inserting typical values,

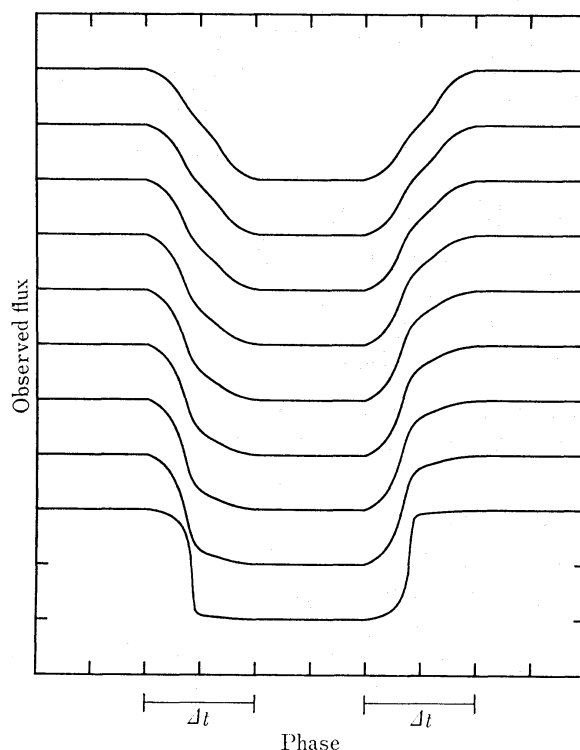


Fig. 5. The dependence of X-ray light curves on the declination angle. From top to bottom $\delta_0 = 90^\circ$ to 10° in steps of 10° .

it takes about 1 s for the inner region of the disk to be eclipsed. In addition, the duration time of the total eclipse is about 10^3 s (Fukue 1987b).

The X-ray astronomical satellite Ginga (meaning galaxy in Japanese) was launched in February 1987. The large-area proportional counter (LAC) aboard Ginga has sensitivity in the 2–30-keV range and a maximum time resolution of 0.98 ms (Makino and the Astro-C team 1987). Hence, the high time resolution of Ginga will easily detect the light-curve asymmetry of the accretion disk around a compact object discussed above, if an eclipse is found. Such an observation will verify the disk model (e.g., the standard model is valid or not) and further bring the space-time information near the compact object (e.g., the compact object rotates or not?).

b. Active Galactic Nuclei

Next we shall briefly mention the accretion disk in active galactic nuclei. As for light curves, it is noted that the results obtained for X-ray light curves in the case of close binary systems discussed in figures 4 and 5 are roughly applicable for the accretion disk around the supermassive black hole in active galactic nuclei, if the X-ray light curves are replaced by the optical-UV light curves. This is because the peak of the spectrum from the disk is not in the X-ray band but in the optical-UV band.

If the disk is eclipsed by a cloud orbiting the supermassive black hole, then the eclipsing time scale becomes

$$\Delta t = 10.4 R p_{\text{pc}}^{1/2} M_8^{1/2} d, \quad (8)$$

where R is again the size of the eclipsing region in units of the Schwarzschild radius,

p_{pc} is the periastron distance of the cloud in units of parsec, and M_8 is the mass of the masssupersive black hole in units of $10^8 M_\odot$. Equation (8) yields a typical time scale of 1 yr.

c. Remarks

In the present analysis, we have used the classical standard model (e.g., Page and Thorne 1974). However, it has been argued that near the marginally stable radius (inner edge) the structure of the disk should be modified from the standard disk, since the almost circularly rotating flow outside this radius should transit to a free falling flow toward the hole through the sonic point (Muchotrzeb 1983; Matsumoto et al. 1984; Fukue 1987a). We must use these models for a more sophisticated treatment.

In calculating the light curves, we have assumed that the vertical obstacle occults the disk. In close binary systems, however, if the declination angle becomes larger, then the curvature of the companion edge should be taken into considerations.

We here set the black hole at the center of the geometrically thin accretion disk. Taking photographs of thin disks around a neutron star or with a hot corona or further of accretion tori with jets are left as future works.

The authors thank Drs. H. Inoue, T. Matsuda, and K. Sadakane and Messrs. M. Okyudo and T. Yokoo for discussions and useful comments. This work was supported in part by a Grant-in-Aid for Scientific Research of the Ministry of Education, Science, and Culture (61740141, 62740145).

Editorial Note: The authors used the term “Lady” for the “accretion disk.” The editors replaced this by the “accretion disk” in accordance with the general style of the *Publications of the Astronomical Society of Japan*. Editors.

References

- Cunningham, C. T. 1975, *Astrophys. J.*, **202**, 788.
 Czerny, B., Czerny, M., and Grindlay, J. E. 1986, *Astrophys. J.*, **311**, 241.
 Fukue, J. 1987a, *Publ. Astron. Soc. Japan*, **39**, 309.
 Fukue, J. 1987b, *Nature*, **327**, 600.
 Gerbal, D., and Pelat, D. 1981, *Astron. Astrophys.*, **95**, 18.
 Luminet, J.-P. 1979, *Astron. Astrophys.*, **75**, 228.
 Lynden-Bell, D. 1969, *Nature*, **223**, 690.
 Makino, F., and the Astro-C team. 1987, *Astrophys. Letters*, **25**, 223.
 Malkan, M. A. 1983, *Astrophys. J.*, **268**, 582.
 Matsumoto, R., Kato, S., Fukue, J., and Okazaki, A. T. 1984, *Publ. Astron. Soc. Japan*, **36**, 71.
 Mitsuda, K., Inoue, H., Koyama, K., Makishima, K., Matsuoka, M., Ogawara, Y., Shibazaki, M., Suzuki, K., Tanaka, Y., and Hirano, T. 1984, *Publ. Astron. Soc. Japan*, **36**, 741.
 Muchotrzeb, B. 1983, *Acta Astron.*, **33**, 79.
 Novikov, I. D., and Thorne, K. S. 1973, in *Black Holes*, ed. C. DeWitt and B. S. DeWitt (Gordon and Breach, New York), p. 343.
 Page, D. N., and Thorne, K. S. 1974, *Astrophys. J.*, **191**, 499.
 Shakura, N. I., and Sunyaev, R. A. 1973, *Astron. Astrophys.*, **24**, 337.